

Supporting information

**Cu-enhanced Photoelectronic and Ethanol Sensing Properties of Cu₂O/Cu Nanocrystals
Prepared by One-step Controllable Synthesis**

Yao Hu;^a Muwei Ji;^{a,b,c} Yiqing He;^a Ziyi Liu;^a Qinghua Yang;^a Chaozheng Li;^d Jiajia Liu;^d Bo Li;^a Jiatao Zhang;^{d,*} Caizhen Zhu;^{b,*} and Jin Wang^{a,*}

a. Graduated school at Shenzhen, Tsinghua University, Shenzhen, 518065, China

b. College of Chemistry and Environment Engineering, Shenzhen University, Shenzhen, 518060, China

c. Institute of Chemistry, Chinese Academy of Sciences, Beijing , 100190, China

d. Beijing Key Laboratory of Construction Tailorable Advanced Functional Materials and Green Applications, School of Materials Science and Engineering, Beijing Institute of Technology, Beijing 100081, China.

Tab. S1 The molar ratio of Cu₂O and Cu in the four samples.

Sample	Cu ₂ O: Cu (molar ratio)
Cu ₂ O (2 mmol A.A.)	∞
Cu ₂ O:Cu (4 mmol A.A.)	5:1
Cu ₂ O:Cu (8 mmol A.A.)	1:4
Cu (12 mmol A.A.)	0

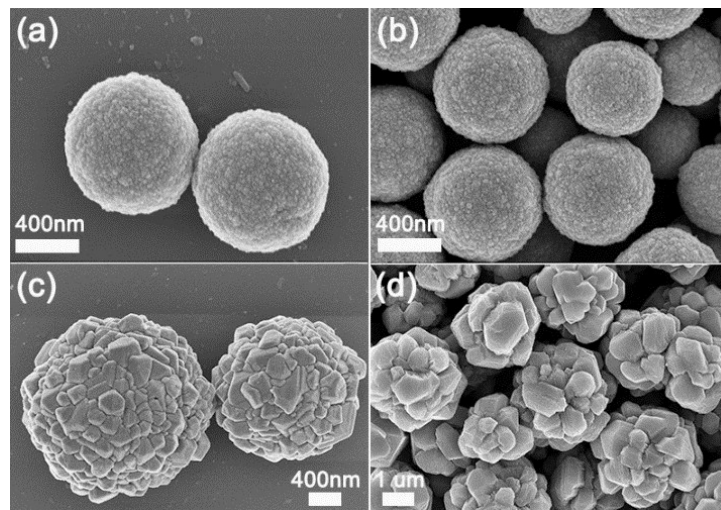


Fig. S1 The SEM images with high magnification for (a) Cu₂O (2 mmol A.A.), (b) Cu₂O/Cu (4 mmol A.A.), (c) Cu₂O/Cu (8 mmol A.A.) and (d) Cu (12 mmol A.A.).

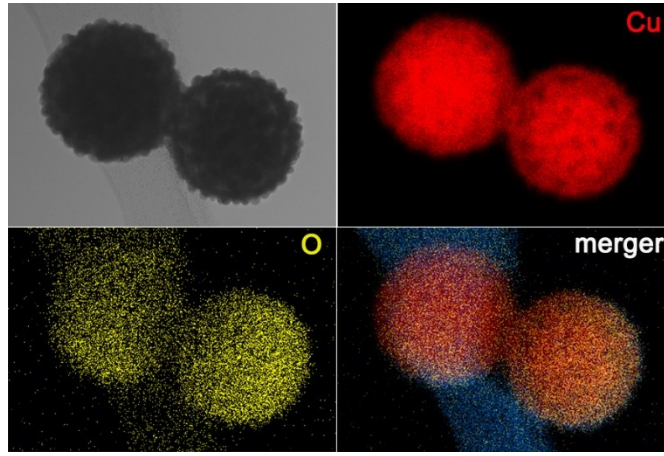


Fig. S2 Elemental mapping of the $\text{Cu}_2\text{O}/\text{Cu}$ structure.

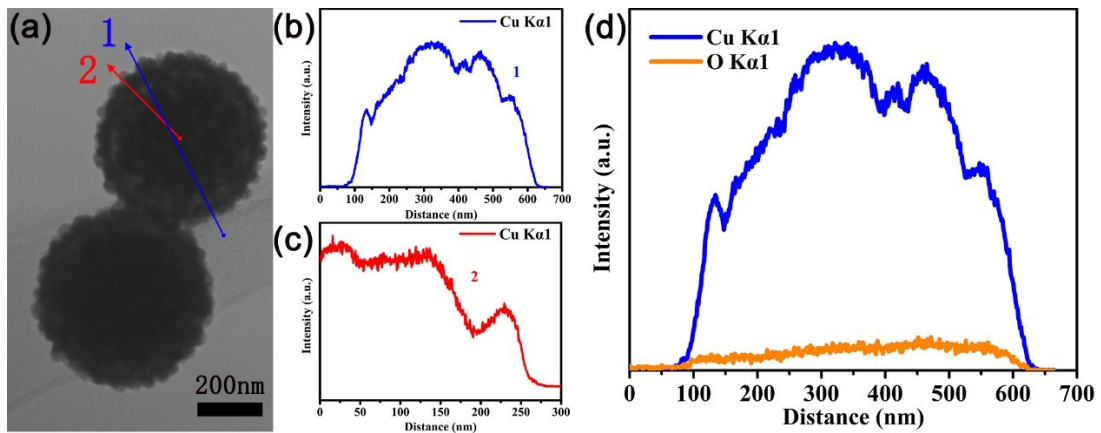


Fig. S3 (a) The LRTEM images of the prepared $\text{Cu}_2\text{O}/\text{Cu}$ particles; (b) and (c) are the concentration of the element copper along the line 1 and 2, respectively; (d) The comparison of Cu and O element intensity along line 1.

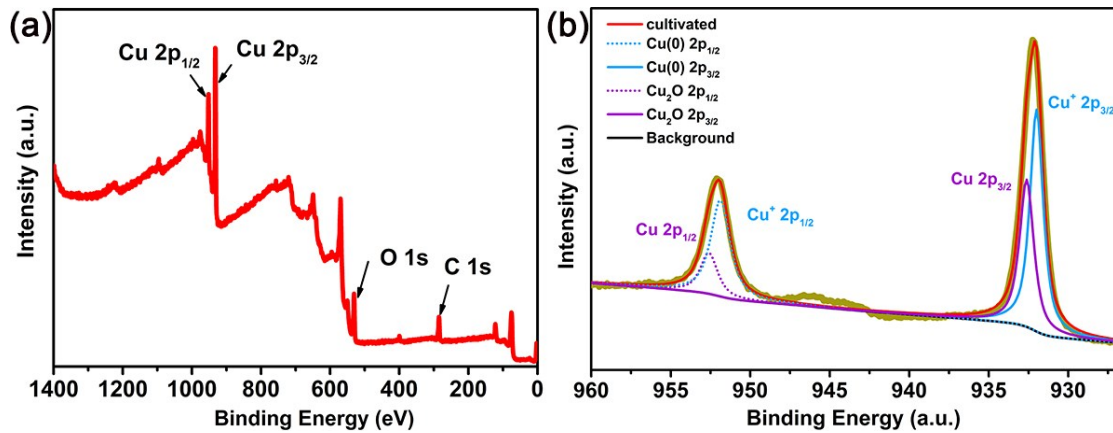


Fig. S4 XPS spectra of the as-prepared samples: (a) overall survey spectra; indicating there are elemental C, O and Cu. Carbon element is attributed to the absorption in the air and the hydrocarbon of the XPS instrument itself. Besides existing in Cu_2O , part of the oxygen element is ascribed to air adsorption like carbon; (b) the Cu XPS peaks of as-prepared $\text{Cu}_2\text{O}/\text{Cu}$.

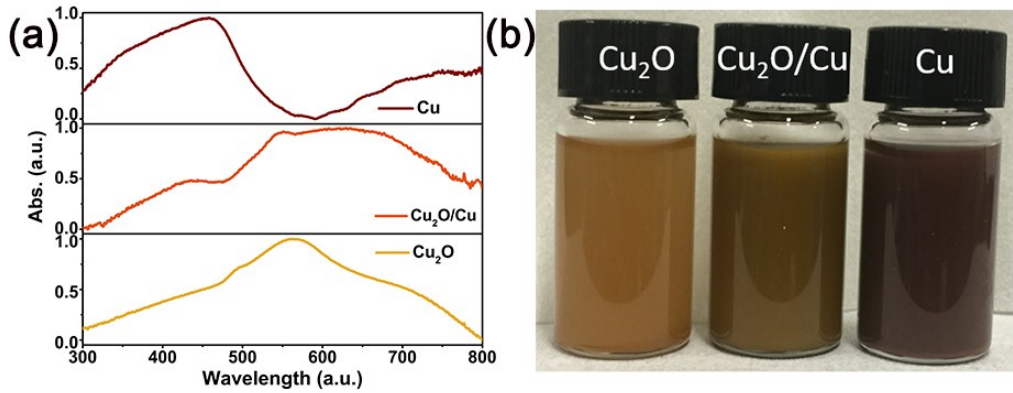


Fig. S5 The UV-vis absorption spectrum (a) and photograph (b) of as-prepared Cu₂O (2 mmol A.A.), Cu₂O/Cu (4 mmol A.A.) and Cu (12 mmol A.A.) nanocrystals.

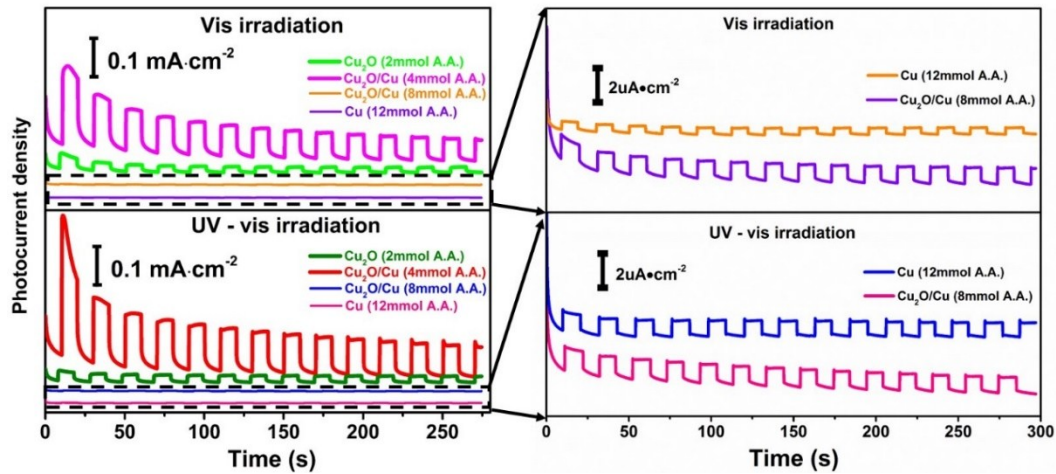


Fig.S6 The photocurrent of Cu-rich Cu₂O/Cu prepared with 8 mmol A.A. and pure Cu prepared with 12 mmol A.A. under UV-vis light and Vis light.

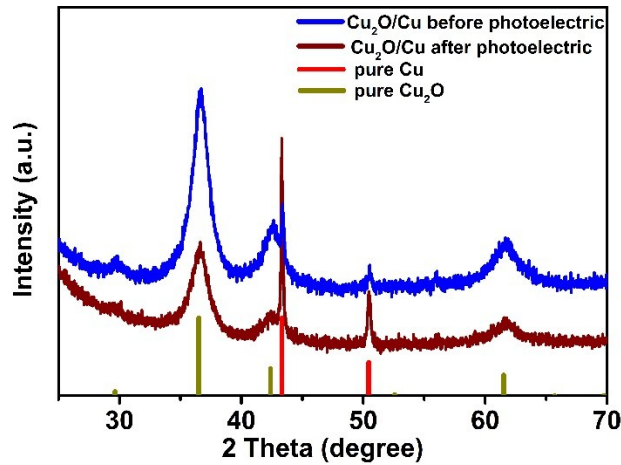


Fig.S7 XRD pattern of Cu₂O/Cu (4 mmol A.A.) before and after UV-vis irradiation.

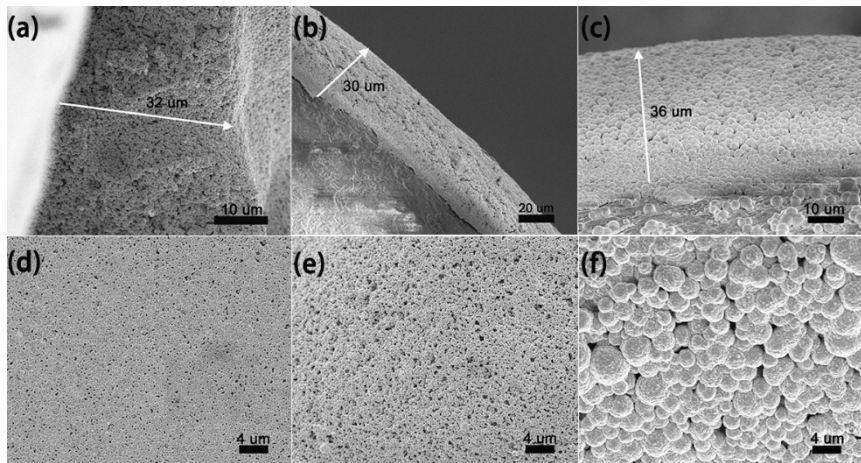


Fig.S8 The sectional SEM image views of (a) Cu_2O (2 mmol A.A.), (b) $\text{Cu}_2\text{O}/\text{Cu}$ (4 mmol A.A.) and (c) $\text{Cu}_2\text{O}/\text{Cu}$ (8 mmol A.A.) after ethanol sensing test; the surface SEM images of (d) Cu_2O (2 mmol A.A.), (e) $\text{Cu}_2\text{O}/\text{Cu}$ (4 mmol A.A.) and (f) $\text{Cu}_2\text{O}/\text{Cu}$ (8 mmol A.A.) after ethanol sensing test.

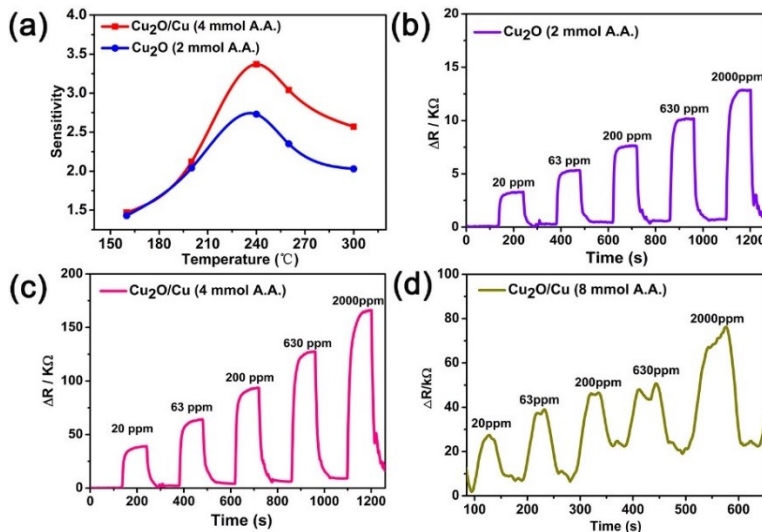


Fig.S9 (a) The relationship of sensitivity and temperature with the ethanol concentration of 200ppm; the resistance for different ethanol gas concentration at 240°C with (b) Cu_2O (2 mmol A.A.), (c) $\text{Cu}_2\text{O}/\text{Cu}$ (4 mmol A.A.) and (d) $\text{Cu}_2\text{O}/\text{Cu}$ (8 mmol A.A.).

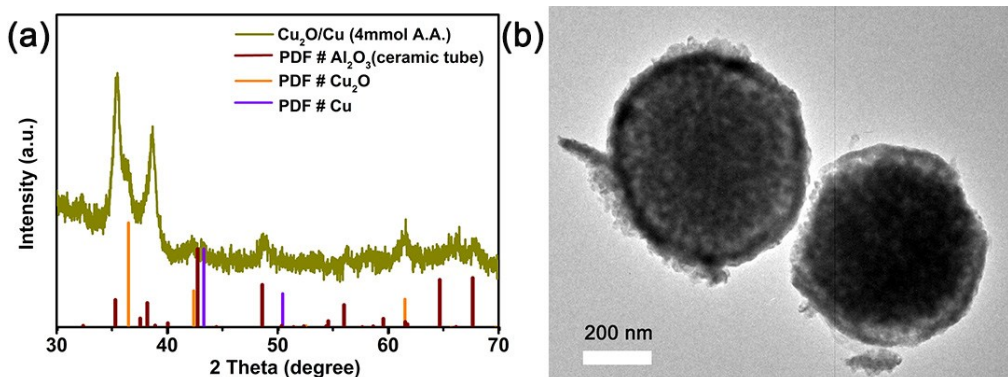


Fig.S10 (a) The XRD pattern of $\text{Cu}_2\text{O}/\text{Cu}$ (4 mmol A.A.) after ethanol sensing test; (b) XRD pattern of $\text{Cu}_2\text{O}/\text{Cu}$ (4 mmol A.A.) after ethanol sensing test.

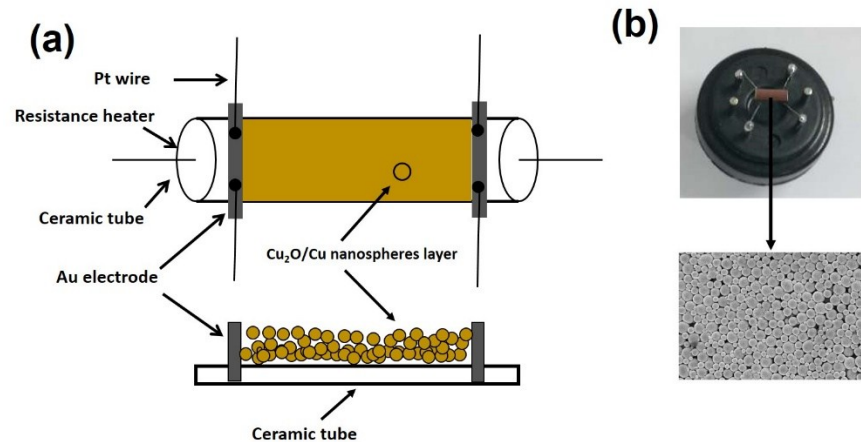


Fig.S11 (a) The photograph of the sensor and the SEM images of pure Cu_2O or $\text{Cu}_2\text{O}/\text{Cu}$ layer; (b) the schematic diagram of the sensor and the sectional view.